C. R. Mecanique 339 (2011) 432–438

Contents lists available at ScienceDirect

Comptes Rendus Mecanique

www.sciencedirect.com

Yield strength of masonry-like structures containing thin adhesive joints: 3D or 2D-interface model for the joints?

Calcul à la rupture des structures de type maçonnerie contenant des joints adhésifs : Un modèle de joint 3D ou 2D?

Ramzi Sahlaoui [a], Karam Sab [b,*], Jean-Vivien Heck [a]

[a] *Centre scientifique et technique du bâtiment (CSTB), 84, avenue Jean-Jaurès, Champs sur Marne, 77447 Marne-la-Vallée cedex 2, France*
[b] *Université Paris-Est, laboratoire Navier (ENPC/IFSTTAR/CNRS, UMR 8205), École des Ponts ParisTech, 6 & 8, avenue Blaise-Pascal, 77455 Marne-la-Vallée cedex 2, France*

ARTICLE INFO

Article history:
Received 31 January 2011
Accepted after revision 25 March 2011
Available online 7 May 2011

Keywords:
Solids and structures
Interface
Adhesive joint
Limit analysis
Homogenization
Masonry
Drucker–Prager

Mots-clés :
Solides et structures
Interface
Joint adhésif
Analyse Limite
Homogénéisation
Maçonnerie
Drucker–Prager

ABSTRACT

It is shown in this Note that the use of a 2D-interface model for the joints in the limit analysis of a structure made of bricks which are bounded with adhesively thin joints leads to an upper bound estimate of the bearing capacities of the structure, as the thickness of the joints goes to zero. Considering the compression in the vertical direction of a running bond masonry made of Drucker–Prager bricks and mortar, it is found that the use of the interface model overestimates by 15 percent the compressive strength of the masonry computed with 3D finite elements. Moreover, comparisons with compression test results show that the damaging behavior of the bricks has an important effect on the actual compressive strength of the masonry.

RÉSUMÉ

On montre dans cette Note que l'utilisation d'un modèle d'interface 2D pour les joints lors de l'analyse limite d'une structure faite de briques assemblées par des joints adhésifs minces conduit à une estimation par excès des capacités portantes de la structure, quand l'épaisseur des joints tend vers zero. Considérant la compression dans le sens vertical d'une maçonnerie constituée de briques et de mortier obéissants au critère de Drucker–Prager, on trouve que l'utilisation du modèle d'interface surestime de 15 pourcent la résistance en compression calculée avec des éléments finis 3D. De plus, des comparaisons avec les résultats de tets de compression montrent que l' endommagement des briques a un effet important sur la résistance en compression de la maçonnerie.

1. Introduction

The use of an interface 2D joint model instead of the full 3D model in the analysis of a structure containing adhesively bonded thin joints is very common in many applications, including masonry-like structures, because the use of small 3D

* Corresponding author.
E-mail addresses: Ramzi.SAHLAOUI@cstb.fr (R. Sahlaoui), sab@enpc.fr (K. Sab), Jean-Vivien.HECK@cstb.fr (J.-V. Heck).

1631-0721/$ – see front matter
doi:10.1016/j.crme.2011.03.018

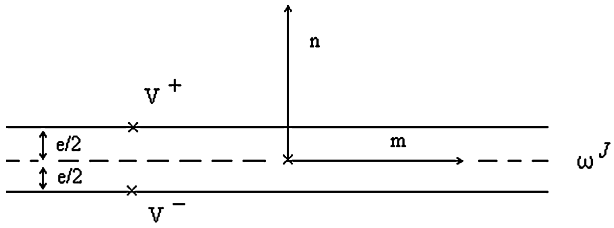

Fig. 1. A plane joint.

finite elements for the joints would be memory and time consuming. This has been fully justified in the elastic case in [1] where asymptotic expansion methods involving two small parameters: the contrast between the joint material and the brick material, and the relative thickness of the joints, where used. Considering the limit analysis of masonry-like structures made of bricks which are bonded with thin joints, the purpose of this Note is to show that the use of an interface 2D model for the joints leads to an upper bound estimate of the bearing capacities of the structure, as the thickness of the joints goes to zero, and to evaluate on an example the discrepancy between the interface 2D model and the full 3D model. Considering the compressive strength in the vertical direction of a running bond masonry made of Drucker–Prager bricks and mortar, the predictions of both the interface and 3D models are computed and compared to experimental results.

2. From 3D to 2D joint model

We study in this Note the limit analysis of a structure made of bricks occupying the domain Ω^B which are bonded with thin joints occupying the domain Ω^J. The strength domain is G^J in the joints, $\mathbf{x} \in \Omega^J$, and G^B in the bricks, $\mathbf{x} \in \Omega^B$. G^J and G^B are two given convex domains of the six-dimensional stress space. Their support functions π^J and π^B are the two positively homogeneous functions of the strain rate symmetric second order tensor $\mathbf{d} = (d_{ij})$, $i, j = 1, 2, 3$, defined by:

$$\pi^\alpha(\mathbf{d}) = \sup_{\boldsymbol{\sigma} \in G^\alpha} \boldsymbol{\sigma} : \mathbf{d}, \quad \boldsymbol{\sigma} \in G^\alpha \quad \Longleftrightarrow \quad \boldsymbol{\sigma} : \mathbf{d} \leqslant \pi^\alpha(\mathbf{d}) \quad \text{for all } \mathbf{d} \tag{1}$$

for $\alpha = J$ or B. The loading of the structure is described by providing (a) the set *KA* of kinematically admissible velocity field vectors $\mathbf{v} = (v_i)$, $i = 1, 2, 3$, with the prescribed boundary conditions; and (b) the linear functional $L(\mathbf{v})$ representing the power of the prescribed external forces. According to the well-known kinematic approach of the yield design theory [2], the structure cannot sustain the loading if there exists a velocity field in *KA* such that:

$$\int_{\Omega^J} \pi^J\big(\nabla \otimes^s \mathbf{v}\big)\,\mathrm{d}\Omega^J + \int_{\Omega^B} \pi^B\big(\nabla \otimes^s \mathbf{v}\big)\,\mathrm{d}\Omega^B < L(\mathbf{v}) \tag{2}$$

where $\nabla \otimes^s \mathbf{v}$ is the symmetric part of the gradient of $\mathbf{v}$.

For the sake of simplicity, only plane joints with uniform thickness are studied in this paper. See Fig. 1. $\mathbf{n}$ is the normal to the middle surface ω^J of the joint, $(\mathbf{l}, \mathbf{m}, \mathbf{n})$ is a local basis, e is the thickness of the joint, $\mathbf{v}^+$ and $\mathbf{v}^-$ are the values of the velocity $\mathbf{v}$ at the joint boundaries. The idea is to consider the following linear interpolation of the velocity in the thickness of the joint:

$$\mathbf{v}(x_l, x_m, x_n) = \frac{\mathbf{v}^+(x_l, x_m) + \mathbf{v}^-(x_l, x_m)}{2} + \frac{\mathbf{v}^+(x_l, x_m) - \mathbf{v}^-(x_l, x_m)}{e} x_n \tag{3}$$

Due to the fact that π^J is positively homogeneous, it can be shown under some regularity conditions on $\mathbf{v}^+$, $\mathbf{v}^-$ and π^J that, fixing ω^J, $\mathbf{v}^+$ and $\mathbf{v}^-$, the limit of the first term of the left-hand side of (2) is finite and is given by:

$$\lim_{e \to 0^+} \int_{\Omega^J} \pi^J\big(\nabla \otimes^s \mathbf{v}\big)\,\mathrm{d}\Omega^J = \int_{\omega^J} \pi^J\big(\mathbf{n} \otimes^s [\mathbf{v}]\big)\,\mathrm{d}\omega^J \tag{4}$$

where $[\mathbf{v}] = \mathbf{v}^+ - \mathbf{v}^-$ is the velocity jump. The right-hand side of (4) is the maximal resistant power of the interface 2D joint model. The interface yield strength domain g^J is the convex domain of the three-dimensional space of stress vector $\mathbf{t} = \boldsymbol{\sigma}.\mathbf{n}$ such that $\boldsymbol{\sigma} \in G^J$. Using standard duality techniques, it is equivalently defined by:

$$\mathbf{t} \in g^J \quad \Longleftrightarrow \quad \mathbf{t}.\mathbf{u} \leqslant \pi^J\big(\mathbf{n} \otimes^s \mathbf{u}\big) \quad \text{for all vectors } \mathbf{u} \tag{5}$$

If the contribution of the interpolated velocity in the joint, (3), to $L(\mathbf{v})$ vanishes, as the thickness of the joints goes to zero, then the above kinematic analysis clearly shows that substituting the interface 2D joint model for the 3D joint model leads asymptotically to an upper bound estimation of the bearing capacities of the structure. Using the same interpolation techniques for the velocity field in the joints, the same conclusion holds true for curved joints with possibly intersecting

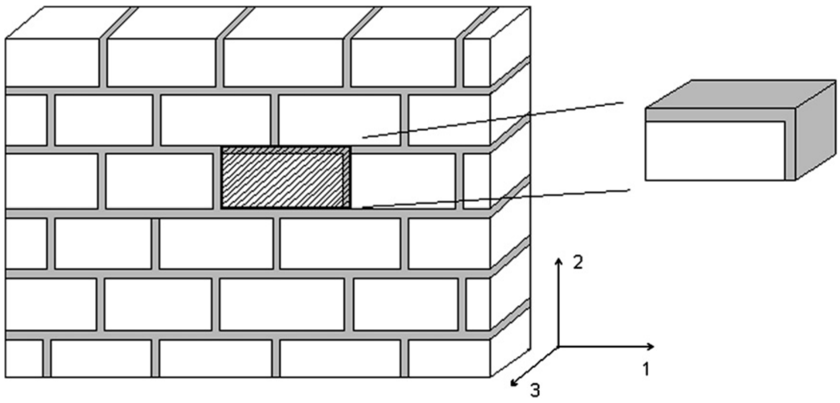

Fig. 2. The running bond masonry geometry and the extracted unit cell.

zones. This result could be easily obtained with the static approach *under the additional assumption* that the bricks are more resistant than the joints: $G^J \subset G^B$. Indeed, in this case, the condition $\boldsymbol{\sigma}(\mathbf{x}) \in G^J$ for $\mathbf{x} \in \Omega^J$ can be relaxed into the conditions $\boldsymbol{\sigma}(\mathbf{x}) \in G^B$ for $\mathbf{x} \in \Omega^J \setminus \omega^J$ and $\boldsymbol{\sigma}(\mathbf{x}).\mathbf{n} \in g^J$ for $\mathbf{x} \in \omega^J$. In other words, in the case $G^J \subset G^B$, an upper bound estimation of the bearing capacities of the structure is obtained for arbitrary thickness of the joints by replacing the joint material with the brick material everywhere except at the middle surface of the joints, ω^J, where the interface yield condition $\boldsymbol{\sigma}.\mathbf{n} \in g^J$ is imposed.

3. The vertical compressive strength of a running bond masonry

The running bond masonry geometry is described in Fig. 2. It is made of identical parallelepipedic bricks (side length b in the horizontal direction 1, a in the vertical direction 2 and t in the third direction) separated by horizontal continuous bed joints and alternate vertical head joints. e_h is the thickness of the horizontal joints, e_v is the thickness of the vertical joints. Bricks and joints are both made of Drucker–Prager materials. The Drucker–Prager yield function is:

$$\boldsymbol{\sigma} \in G \quad \Longleftrightarrow \quad f(\boldsymbol{\sigma}) \leqslant \mathbf{0} \quad \text{with } f(\boldsymbol{\sigma}) = q + p \tan\beta - c \tag{6}$$

where $p = \frac{1}{3}tr(\boldsymbol{\sigma})$ is the hydrostatic stress, $\mathbf{s} = \boldsymbol{\sigma} - p\mathbf{I}$ is the deviatoric stress, $q = \sqrt{\frac{3}{2}\mathbf{s}:\mathbf{s}}$, $c > 0$ is the Drucker–Prager cohesion and β is the Drucker–Prager friction angle with $(c, \beta) = (c^J, \beta^J)$ in the joints and $(c, \beta) = (c^B, \beta^B)$ in the bricks. According to [2], the Drucker–Prager interface yield strength defined by (5) coincides with the Mohr–Coulomb one given by:

$$\tau + \sigma \tan\varphi - c' \leqslant 0 \tag{7}$$

where σ is the normal component of $\boldsymbol{\sigma}.\mathbf{n}$, $\sigma = \mathbf{n}.(\boldsymbol{\sigma}.\mathbf{n})$, τ is its shear component $|\boldsymbol{\sigma}.\mathbf{n} - \sigma\mathbf{n}|$, φ is the Mohr–Coulomb friction angle such as $\frac{3\sin\varphi}{\sqrt{3+\sin^2\varphi}} = \tan\beta$ and $c' = c\tan\varphi/\tan\beta$ is the Mohr–Coulomb cohesion.

The corresponding π-function writes:

$$\pi\left(\mathbf{n} \otimes^s [\mathbf{v}]\right) = \begin{cases} (c'/\tan\varphi)[\mathbf{v}].\mathbf{n} & \text{if } [\mathbf{v}].\mathbf{n} \geqslant |[\mathbf{v}]|.\sin\varphi \\ +\infty & \text{otherwise} \end{cases}$$

where $[\mathbf{v}]$ is the velocity jump across the joint interface ω^J.

According to the homogenization method for the limit analysis of thin periodic plates, first proposed by Bourgeois [3] and then independently by Sab [4] and Dallot and Sab [5], the overall compressive strength in the vertical direction, Σ_c, of the considered masonry is determined as follows. Let Y denotes an elementary unit cell which contains all information necessary to completely describe the periodic plate both in directions 1 and 2. This cell is denoted by:

$$Y = A \times \left]-\frac{t}{2}, \frac{t}{2}\right[$$

where $A \subset \mathbb{R}^2$ is the middle section of Y in the $(1,2)$-plane; The plate unit cell problem is actually different from the well-known unit cell problem for 3D periodic media. The main differences concern the boundary conditions. Indeed, let the boundary ∂Y of Y be decomposed into three parts:

$$\partial Y = \partial Y_l \cup \partial Y_3^+ \cup \partial Y_3^-, \quad \text{with } \partial Y_3^\pm = A \times \left\{\pm\frac{t}{2}\right\}$$

Periodic boundary conditions will be imposed to the lateral boundary ∂Y_l while stress free boundary conditions will be imposed to $\partial Y_3^{\pm}$. Taking into account the symmetries of the microstructure, [5,6], the static determination of Σ_c is as follows: find the maximum value of Σ such that there exists a stress field $\boldsymbol{\sigma} = (\sigma_{ij})$ of the unit cell Y verifying:

$$\begin{aligned} &\boldsymbol{\sigma}(\mathbf{y}) \in G(\mathbf{y}), \quad \forall \mathbf{y} \in Y \\ &\langle \sigma_{11} \rangle = \langle \sigma_{12} \rangle = 0, \qquad \langle \sigma_{22} \rangle = -\Sigma \\ &\operatorname{div} \boldsymbol{\sigma} = 0 \quad \text{on } Y \\ &\boldsymbol{\sigma} \cdot \mathbf{n} \ \text{skew-periodic on } \partial Y_l; \qquad \boldsymbol{\sigma} \cdot \mathbf{e}_3 = 0 \quad \text{on } \partial Y_3^{\pm} \end{aligned} \tag{8}$$

where $\langle \cdot \rangle$ is the volume average on Y. It can be shown that the average out-of-plane components $\langle \sigma_{i3} \rangle$, $i = 1, 2, 3$ of $\boldsymbol{\sigma}$ in (8) are null. However, $\boldsymbol{\sigma}$ is not a plane stress field in the general case.

According to [5,6], the kinematic definition of Σ_c is obtained by considering the set of kinematically compatible velocity fields of the unit cell, $\mathbf{v} = (v_i)$ defined by:

$$KA(\mathbf{D}) = \left\{ \mathbf{v} \,\middle|\, \nabla \otimes^s \mathbf{v} = \mathbf{D} + \nabla \otimes^s \mathbf{u}^{per},\ \mathbf{u}^{per}\ A\text{-periodic in } (1, 2) \right\} \tag{9}$$

where $\mathbf{D} = (D_{ij})$, $D_{i3} = 0$, $i, j = 1, 2, 3$ is the in-plane part of the macroscopic strain.

$$\Sigma_c = \inf_{\mathbf{v} \in KA(\mathbf{D}),\, D_{22} = -1} \left\langle \pi\left(\nabla \otimes^s \mathbf{v} \right) \right\rangle \tag{10}$$

In the general case, $\mathbf{u}^{per}(y_1, y_2, y_3)$ has three components ($u_3 \neq 0$) and it is periodic only in the directions 1 and 2. Hence, the average out-of-plane components of $\mathbf{d} = \nabla \otimes^s \mathbf{v}$ for $\mathbf{v} \in KA(\mathbf{D})$ are not null. We have $\langle d_{\alpha\delta} \rangle = D_{\alpha\delta}$, $\alpha, \delta = 1, 2$, and $\langle d_{i3} \rangle \neq 0$, $i = 1, 2, 3$. So, in the general case, the 3D unit cell problem (8)–(10) is not a plane stress one nor a plane strain one.

If the interface 2D joint model is substituted for the 3D joint model in the above described limit analysis problem, then the first condition in (8) becomes $\boldsymbol{\sigma}(\mathbf{y}) \in G^B$ for all $\mathbf{y}$ in Y^*, and $\mathbf{t}(\mathbf{y}) \in g^J$ for all $\mathbf{y}$ located at the interface ω^J between the bricks. The maximum value of Σ is noted Σ_c^*. Here, Y^* is the unit cell obtained from Y by setting $e_h = e_v = 0$. G^B is given by (6) with $(c, \beta) = (c^B, \beta^B)$ and g^J is given by (7) with $(c, \beta) = (c^J, \beta^J)$. Moreover, Σ_c^* can be computed using the kinematic approach (10) where the average $\langle \pi \rangle$ becomes $\langle \pi^B(\nabla \otimes^s \mathbf{v}) \rangle + \frac{1}{|Y^*|} \int_{\omega^J} \pi^J(\mathbf{n} \otimes^s [\mathbf{v}])\, \mathrm{d}\omega^J$. In the case of infinitely resistant bricks with rigid body kinematics, this 3D unit cell problem with 2D-interface joint model coincides with the one introduced by de Buhan and de Felice [7].

We claim that if the joints are modeled as 2D interfaces as described above, then the vertical compressive strength of the running bond masonry is equal to the compressive strength of the bricks, Σ_c^B, i.e. $\Sigma_c^* = \Sigma_c^B$. Indeed, consider the uniform stress field in Y^*: $\sigma_{22} = -\Sigma$, $\sigma_{ij} = 0$ for all $(i, j) \neq (2, 2)$, in the static approach. It is clear that the balance equation, the static boundary conditions, the averaging condition and the interface condition are verified for all $\Sigma > 0$. Hence, the maximum compatible value of Σ is Σ_c^B, and we have $\Sigma_c^B \leqslant \Sigma_c^*$. Moreover, using the following continuous velocity field $D_{12} = 0$, $u_1^{per}(\mathbf{y}) = u_2^{per}(\mathbf{y}) = 0$, $u_3^{per}(\mathbf{y}) = D_{11} y_3$ in the kinematic approach, we have

$$\mathbf{d} = \nabla \otimes^s \mathbf{v} = \begin{pmatrix} D_{11} & 0 & 0 \\ 0 & -1 & 0 \\ 0 & 0 & D_{11} \end{pmatrix}$$

and optimizing (10) over D_{11} leads to $\Sigma_c^* \leqslant \Sigma_c^B$.

4. Finite elements computations

The limit analysis problem with 3D joints has been solved on the unit cell of Fig. 2 with the ABAQUS finite elements software. Elasto-plastic simulations with perfectly plastic Drucker–Prager materials (no hardening) obeying the normality rule were performed with the following material constants for the brick and the joints, respectively: Young's modulus, 6740 Mpa and 1700 Mpa; Poisson's ratio, 0.167 and 0.06; β, 30° and 40°; c, 4.328 Mpa and 0.348 Mpa. Actually, the ABAQUS software may exhibit some convergence problems due to the non-differentiability of the Drucker–Prager yield function at $q = 0$. Hence, a regularized (hyperbolic) version of the Drucker–Prager yield function has been used where $\sqrt{l_0^2 + q^2}$ is substituted for q in (6). Here, l_0 is a small positive constant compared to the cohesion (0.022 Mpa in the brick and 0.002 Mpa in the joints).

The periodicity conditions on the lateral boundary of the unit cell have been imposed by matching the degrees of freedom of the pairs of nodes situated on these boundaries as follows:

$$\mathbf{v}(\mathbf{y}_E) - \mathbf{v}(\mathbf{y}_B) = \mathbf{D}.(\mathbf{y}_E - \mathbf{y}_B) = \begin{pmatrix} (\frac{b+e_v}{2})D_{11} + (a + e_h)D_{12} \\ (\frac{b+e_v}{2})D_{12} + (a + e_h)D_{22} \\ 0 \end{pmatrix}$$

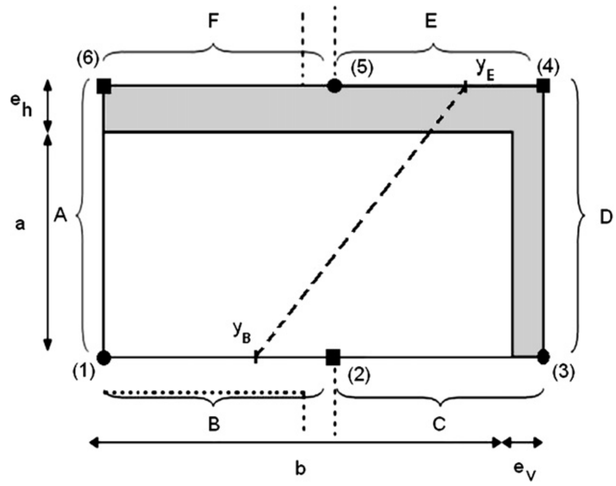

Fig. 3. The periodicity conditions.

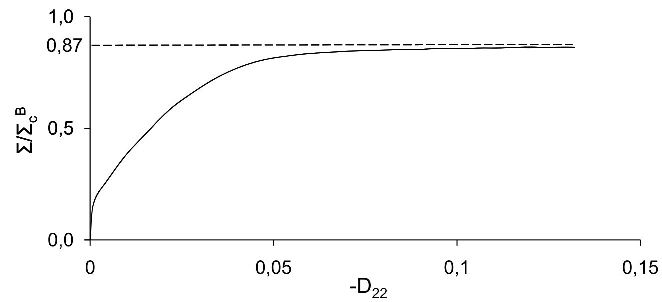

Fig. 4. The normalized stress–strain curve and the determination of the compressive strength.

$$\mathbf{v}(\mathbf{y}_D) - \mathbf{v}(\mathbf{y}_A) = \mathbf{D}.(\mathbf{y}_D - \mathbf{y}_A) = \begin{pmatrix} (b+e_v)D_{11} \\ (b+e_v)D_{12} \\ 0 \end{pmatrix}$$

$$\mathbf{v}(\mathbf{y}_F) - \mathbf{v}(\mathbf{y}_C) = \mathbf{D}.(\mathbf{y}_F - \mathbf{y}_C) = \begin{pmatrix} -(\frac{b+e_v}{2})D_{11} + (a+e_h)D_{12} \\ -(\frac{b+e_v}{2})D_{12} + (a+e_h)D_{22} \\ 0 \end{pmatrix} \tag{11}$$

where A, B, C, D, E, F are the six faces of the lateral boundary shown in Fig. 3 where a section in the $(1,2)$-plane of the unit cell is represented. This can be justified as follows: for example, the infinite microstructure is obviously kept invariant if translated by the vector joining node (1) to node (5). Hence, face E, which is the image of face B by this translation should me matched by periodicity conditions with face B. The six nodes (k) with $k = 1, 2, \ldots, 6$, match as follows: (4) with (6) and (2); (5) with (1) and (3). Using the above equations, it is possible to express the **D** components in terms of the degrees of freedom, $\mathbf{v}^{(k)}$, of these nodes. Indeed, setting $\mathbf{v}^{(1)} = 0$, we obtain

$$D_{11} = \frac{v_1^{(3)}}{b+e_v}, \qquad D_{12} = \frac{v_2^{(3)}}{b+e_v}, \qquad D_{22} = \frac{v_2^{(5)} - 0.5v_2^{(3)}}{a+e_h} \tag{12}$$

These equations are inserted in the periodic conditions (11) so that these conditions become linear relations between the nodal degrees of freedom of the lateral boundary of the unit cell. The "Equation" feature of ABAQUS is used to implement these relations and the loading parameter $-D_{22}$ is increased from zero until the flow of the structure occurs. The overall vertical compressive stress $\Sigma = -\langle\sigma_{22}\rangle$ is computed by averaging the stress values at the Gauss points. Fig. 4 shows the obtained stress–strain curve from which the vertical compressive strength Σ_c is obtained as the asymptotic value of Σ. We have found $\Sigma_c \approx 0.87\Sigma_c^B$. In our simulations, the $C3D8$ ABAQUS 8-node element has been used with three elements in the joint thickness. Fig. 5a shows the mesh details in the in-plane directions. The thickness of the cell in the third direction is 10 mm. Actually, the brick is plastically deformed by compression except in the central zone situated between the vertical joints as shown in Fig. 5b where the stress σ_{33} is represented. Its average value in the joint is nearly equal to −2 Mpa while it is very small in the brick. Hence, $\boldsymbol{\sigma}$ is not a plane stress field. Moreover, it is clear from Fig. 5b that the collapse mode is not a plane strain one.

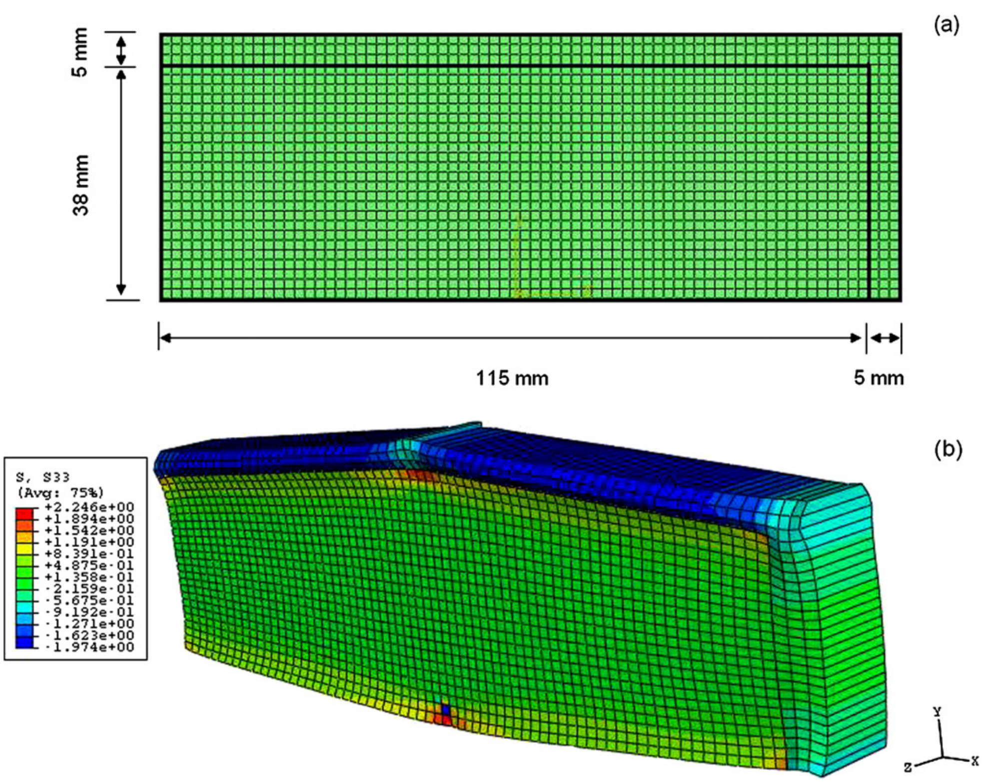

Fig. 5. (a) The mesh details in the in-plane directions; (b) the plastic collapse mode and σ_{33}.

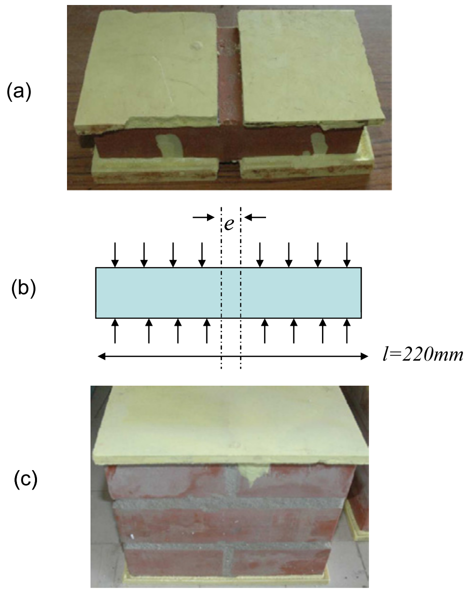

Fig. 6. Compression tests. (a) Partially compressed brick specimen; (b) loading conditions on the partially compressed brick; (c) three-layer masonry specimen.

5. Experimental results

The strength of full clay bricks under compression tests was measured. Three compression test configurations have been considered: (i) uniform compression of one single brick on its upper and lower faces; (ii) partial compression of one single brick on its upper and lower faces *except at the location of the vertical joints* as shown in Figs. 6a and 6b; (iii) uniform compression of the three-layer running bond structure shown in Fig. 6c. The dimensions of the bricks were 220 mm ×

105 mm × 50 mm. Two values for the joint thickness have been considered in the configurations (ii) and (iii): $e = 5$ mm and $e = 20$ mm. For each configuration and each e, three samples have been tested. The strength of a tested specimen is the ratio of the applied force at failure over its bed area (23 100 mm^2).

The uniform compressive strength of the brick in the configuration (i), Σ_c^B, ranges between 72 Mpa and 101 Mpa with an average value of 86 Mpa. The authors are aware that the number of tested specimen (3) does not allow for accurate quantitative estimation of the average compressive strength. Hence, the following results should be considered as qualitative. Nevertheless, it was found that e has no significant effect on the compressive strength measured in the configurations (ii) and (iii). It ranges between 53 Mpa and 66 Mpa with an average value of 61 Mpa (71% of Σ_c^B) in the configuration (ii), and between 38 Mpa and 49 Mpa with an average value of 44 Mpa (51% of Σ_c^B) in the configuration (iii). The later result is consistent with [8] where the compressive strength of the running bond masonry in the vertical direction is 58% of the compressive strength of the bricks.

Now, consider the partially compressed brick of Figs. 6a and 6b – configuration (ii) – and the piecewise uniform vertical compressive stress field taking null value at the central zone of the specimen and Σ_c^B value elsewhere. This stress field being statically and plastically compatible, the strength of the partially compressed specimen should be greater or equal to $(1 - e/l)\Sigma_c^B$ ($\geqslant 0.91\Sigma_c^B$) according to the static approach of limit analysis. The actual strength being 71% of Σ_c^B, this test exhibits the gap between the real damaging behavior of the brick and limit analysis.

In conclusion, we have shown that the use of an interface 2D joint model in the limit analysis of a structure containing adhesively bonded thin joints leads to an upper bound estimate of the bearing capacities of the structure, as the thickness of the joints goes to zero. We have evaluated the discrepancy between the 2D joint model and full 3D finite elements for the determination of the compressive strength of a running bond masonry. Indeed, in this case, the prediction of the 2D joint model is analytical and coincides with the compressive strength of the bricks, Σ_c^B. For a small thickness joint to brick size ratio $e/l = 0.04$, it is found that the full 3D finite element model is 87% of the 2D joint one. Moreover, compression tests have shown that the actual vertical compressive strength of the masonry is about 51% of Σ_c^B, and that the strength of a partially compressed brick is 71% of Σ_c^B. Hence, there are three explaining effects for the difference between the actual vertical compressive strength of the masonry and the compressive strength of the brick: the 3D effect of the joints, the damaging behavior of the bricks and the kinematics of the tested masonry sample which is not rigorously periodic in the in-plane directions.

References

[1] A. Cecchi, K. Sab, A multi-parameter homogenization study for modelling elastic masonry, Eur. J. Mech. A/Solids 21 (2002) 249–268.
[2] J. Salençon, Calcul à la Rupture et Analyse Limite, Presses de l'Ecole Nationale des Ponts et Chaussées, Paris, 1983.
[3] S. Bourgeois, Modélisation numérique des panneaux structures lé gers, PHD thesis, Université Aix-Marseille II, 1997.
[4] K. Sab, Yield design of thin periodic plates by a homogenization technique and an application to masonry walls, C. R. Mécanique 331 (2003) 641–646.
[5] J. Dallot, K. Sab, Limit analysis of multi-layered plates. Part I: The Love–Kirchhoff model, J. Mech. Phys. Solids 56 (2008) 561–580.
[6] K. Sab, A. Cecchi, J. Dallot, Determination of the overall yield strength domain of out-of-plane loaded brick masonry, International Journal of Multiscale Computational Engineering 5 (2007) 83–92.
[7] P. de Buhan, G. de Felice, A homogenization approach to the ultimate strength of brick masonry, J. Mech. Phys. Solids 45 (7) (1997) 1085–1104.
[8] A.W. Page, The strength of brick masonry under biaxial tension-compression, Int. J. Masonry Constr. 3 (1) (1983) 26–31.